Dalton Transactions

Accepted Manuscript

ROYAL SOCIETY OF CHEMISTRY

www.rsc.org/dalton

Journal Name

RSCPublishing

ARTICLE

Acetato-bridged dinuclear lanthanide complexes with single molecule magnet behaviour for the Dy_2 species

Cite this: DOI: 10.1039/xoxxoooooox

Haixia Zhang,[a,b] Shuang-Yan Lin,[a,b] Shufang Xue,[a,b] Chao Wang[a] and Jinkui Tang*[a]

Received ooth January 2012,
Accepted ooth January 2012

DOI: 10.1039/xoxxoooooox

www.rsc.org/

Five dinuclear lanthanide complexes with formula $[Ln_2L_2(OAc)_4(MeOH)_a(H_2O)_b]\cdot cMeOH\cdot dH_2O$ (a = 2, b = 0, c = 2, d = 0, Ln = Sm (**1**), Gd (**2**), Dy (**3**); a = 0, b = 2, c = 4, d = 2, Ln = Tm (**4**)) and $[Yb_2L_2(OAc)_4(MeOH)_2]\cdot[Yb_2L_2(OAc)_4(H_2O)_2]\cdot 2H_2O$ (**5**) (HL = (E)-N'-(2-hydroxybenzylidene)-2-mercaptonicotinohydrazide), have been synthesized and their crystal structures and magnetic properties are reported. All five complexes are centrosymmetric, showing similar dinuclear core with two lanthanide ions in each complex being bridged by acetate groups in the form of $\eta^1:\eta^2:\mu_2$ mode. The various coordination modes of acetate groups result in two kinds coordination geometries for Ln ions with the ones in complexes **1**-**4** and the Yb2 in **5** are nine-coordinated with mono-capped square antiprism geometry, while Yb1 ions in the other part of complex **5** are eight-coordinated with triangular dodecahedron geometry. Magnetic susceptibility studies reveal that complex **3** shows single molecule magnet behaviour with energy barrier of 39.1 K. In addition, the comparison of the structural parameters among the similar Dy_2 SMMs with $\eta^1:\eta^2:\mu_2$ coordination mode of carboxylate groups reveals the significant role played by coordination geometry in modulating the relaxation dynamics of SMMs.

Introduction

Since the discovery of the molecule $[Mn_{12}O_{12}(CH_3COO)_{16}(H_2O)_4]$ $(Mn_{12}OAc)$[1] that shows slow relaxation of magnetization at liquid-helium temperatures, in the early 1990s, great increments of compounds displaying this property, known as single-molecule magnets (SMMs), have been reported.[2] The research enthusiasm of scientists promoting the exploration of such advanced magnetic materials is due to their various promising applications in many significant areas such as high-density data storage,[1b, 3] quantum information processing systems,[4] and spintronic devices.[5] Initially, the research was only limited to the field of 3d metal-based[6] complexes, however, compared to 3d metal ions included in most SMMs, lanthanide (Ln) ions are more suitable for constructing high performance SMMs because of their inherent large unquenched orbital angular momentum,[7] which may bring significant anisotropy[8] to the systems. Thus, attention has been given to incorporate 4f ions into SMMs so as to build either heterometallic 3d-4f[9] or homometallic 4f[2c, 10] clusters. Hitherto, lanthanide SMMs continue to flourish in this domain and new high relaxation barriers are being reached.[11] At the same time, it is responsible for researchers to search for more breakthrough outcomes in the case of Ln_n (n = 1, 2, 3, 4, 5 and so on) complexes.[2c, 10b, 10c, 11d, 12] Of particular interest are dinuclear systems with facile control of the intradimer magnetic interactions, especially Dy_2 complexes.[11b, 13] Among them, Dy_2 bridged by carboxylic acid groups[14] have been investigated. It is necessary to prepare some complexes with similar structure by modifying functional group to probe into the structure-property relationship.[15]

It is critical to select suitable organic ligands to gain SMMs with defined geometries and particular properties.[15-16] Earlier, various Schiff base ligands have been utilized in our group, which exhibit excellent performance in the construction of molecules displaying distinct anisotropic centres.[17] In the present study, we choose a new salicylaldehyde-based Schiff base ligand, namely (E)-N'-(2-hydroxybenzylidene)-2-mercaptonicotinohydrazide (HL, Scheme 1). The ligand provides O,N,O-based multichelating sites forming a coordinate pocket, which is especially favorable for accommodating lanthanide ion.[18] Additionally, lanthanide acetates are brought into the systems in the view of enriching the coordination modes by utilizing multidentate acetate groups. Thus, a series of Ln_2 (Ln = Sm (**1**), Gd (**2**), Dy (**3**), Tm (**4**), Yb (**5**)) complexes bridged by acetate groups in the form of $\eta^1:\eta^2:\mu_2$ mode were obtained. Furthermore, the structure-property relationship was primarily discussed through the comparison of the structural parameters of the title Dy_2 complex with that of Dy_2 complex containing n-butyric acid ligand.

Experimental Section

General

All chemicals were of reagent grade and used without further purification. Elemental analysis for C, H, and N were carried out on a Perkin-Elmer 2400 analyzer. FTIR spectra were recorded with a Perkin-Elmer Fourier transform infrared spectrophotometer using the reflectance technique (4000-300 cm^{-1}). Samples were prepared as KBr disks. Magnetic susceptibility measurements were performed in the temperature range 1.9-300 K, using a Quantum Design MPMS XL-7 SQUID magnetometer equipped with a 7 T magnet. The magnetisation isotherm was collected between 0 and 7 T. The diamagnetic corrections for the complexes were estimated using Pascal's constants,[19] and magnetic data were corrected for diamagnetic contributions of the sample holder.

X-Ray crystal structure determinations

Suitable single crystals for complexes **1**-**5** were selected for single-crystal X-ray diffraction analysis. Crystallographic data were collected at a temperature of 293(2) K on a Bruker Apex II CCD diffractometer with graphite monochromated Mo-Ka radiation (λ = 0.71073 Å). Data processing was accomplished with the SAINT processing program. The structure was solved by direct methods and refined on F^2 by full-matrix least squares using SHELXTL97.[20] The location of Ln (Ln = Sm, Gd, Dy, Tm, Yb) atom was easily determined, and S, O, N, and C atoms were subsequently determined from the difference Fourier maps. The non-hydrogen atoms were refined anisotropically. CCDC 972393−972397 contain the supplementary crystallographic data for this paper. These data can be obtained free of charge from The Cambridge Crystallographic Data Centre via www.ccdc.cam.ac.uk/data_request/cif.

Synthesis of the ligand HL

The Schiff-base ligand HL was synthesized by a condensation reaction between salicylaldehyde and 2-mercaptonicotinohydrazide. The crude product was obtained as a pale yellow powder in 75%. Recrystallisation from dimethylformamide and ethanol gave the purified product. Elemental analysis (%) calcd for $C_{13}H_{11}N_2O_2S$: C 60.16, H 4.24, N 10.80; found C 59.66, H 4.19, N 10.71. IR (KBr, cm^{-1}): 3185 (w), 3078 (w), 3008 (w), 2793 (w), 1662 (s), 1621 (m), 1608 (w), 1574 (m), 1545 (s), 1482 (m), 1442 (w), 1357 (w), 1332 (w), 1311 (s), 1278 (m), 1228 (s), 1190 (w), 1155 (m), 1129 (w), 1117 (w), 1082 (m), 1061 (w), 1031 (w), 999 (w), 943 (w), 886 (m), 876 (s), 850 (w), 812 (s), 783 (w), 754 (s), 720 (m), 706 (m), 678 (s), 662 (s), 635 (w), 565 (m), 529 (m).

Synthesis of the complexes

$[Sm_2L_2(OAc)_4(MeOH)_2]\cdot 2MeOH$ (1)

$Sm(OAc)_3\cdot 6H_2O$ (0.1 mmol, 43.56 mg) was reacted with HL (0.1 mmol, 25.93 mg) in MeOH/CH_3CN (15 mL/10 mL) in the presence of triethylamine (abbreviated as Et_3N, 0.15 mmol, 0.15 mL). The ensuing yellow solution was stirred for 5 h and subsequently filtered. The filtrate was left undisturbed to allow the slow volatilization of the solvent. Yellow block-shaped single crystals of complex **1**, suitable for X-ray diffraction analysis, formed after ten days. Yield: 25 mg (41%, based on the metal salt). Elemental analysis (%) calcd for $C_{38}H_{48}Sm_2N_6O_{16}S_2$: C 37.73, H 4.00, N 6.95; found C 37.52, H 3.92, N 6.86. IR (KBr, cm^{-1}): 1610 (m), 1575 (w), 1536 (s), 1470 (w), 1434 (s), 1405 (w),1382 (m), 1328 (m), 1305 (m), 1235 (w), 1205 (w), 1150 (m), 1124 (m),1075 (w), 1020 (w), 974 (w), 937 (w), 888 (m), 852 (w), 804 (w), 759 (m), 750 (w), 736 (w), 708 (w), 673 (s).

$[Gd_2L_2(OAc)_4(MeOH)_2]\cdot 2MeOH$ (2)

$Gd(OAc)_3\cdot 6H_2O$ (0.1 mmol, 44.24 mg) was reacted with HL (0.1 mmol, 25.93 mg) in MeOH/DMF (15 mL/2 mL) in the presence of Et_3N (0.1 mmol, 0.1 mL). The ensuing yellow solution was stirred for 5 h and subsequently filtered. The filtrate was left undisturbed to allow the slow volatilization of the solvent. Yellow block-shaped single crystals of complex **2**, suitable for X-ray diffraction analysis, formed after one week. Yield: 15 mg (24%, based on the metal salt). Elemental analysis (%) calcd for $C_{38}H_{48}Gd_2N_6O_{16}S_2$: C 37.02, H 3.99, N 6.87; found C 37.30, H 4.02, N 6.81. IR (KBr, cm^{-1}): 3114 (w), 1608 (m), 1584 (m), 1537 (s), 1431 (s), 1380 (m), 1339 (m), 1310 (m), 1232 (m), 1185 (m), 1150 (m), 1127 (m), 1083 (w), 1064 (w), 1037 (w), 1019 (w), 967 (w), 932 (w), 890 (m), 863 (w), 799 (w), 761 (m), 745 (s), 698 (s), 666 (s), 630 (m), 610 (w), 588 (s), 542 (w).

$[Dy_2L_2(OAc)_4(MeOH)_2]\cdot 2MeOH$ (3)

$Dy(OAc)_3\cdot 6H_2O$ (0.1 mmol, 44.77 mg) was reacted with HL (0.1 mmol, 25.93 mg) in MeOH/DMF (20 mL/2 mL) in the presence of Et_3N (0.15 mmol, 0.15 mL). The ensuing yellow solution was stirred for 5 h and subsequently filtered. The filtrate was left undisturbed to allow the slow volatilization of the solvent. Yellow block-shaped single crystals of complex **3**, suitable for X-ray diffraction analysis, formed after two weeks. Yield: 18 mg (30%, based on the metal salt). Elemental analysis (%) calcd for $C_{38}H_{48}Dy_2N_6O_{16}S_2$: C 36.99, H 3.92, N 6.81; found C 36.72, H 3.84, N 6.79. IR (KBr, cm^{-1}): 1609 (w), 1530 (s), 1432 (s), 1339 (w), 1309 (w), 1232 (m), 1187 (m), 1150 (m), 1126 (m), 1019 (w), 933 (w), 890 (m), 843 (w), 799 (m), 761 (m), 746 (m), 655 (s).

$[Tm_2L_2(OAc)_4(H_2O)_2]\cdot 4MeOH\cdot 2H_2O$ (4)

$Tm(OAc)_3\cdot 6H_2O$ (0.1 mmol, 45.mg) was reacted with HL (0.1 mmol, 25.93 mg) in MeOH/DMF (20 mL/2 mL) in the presence of Et_3N (0.15 mmol, 0.15 mL). The ensuing yellow solution was stirred for 5 h and subsequently filtered. The filtrate was left undisturbed to allow the slow volatilization of the solvent. Yellow block-shaped single crystals of complex **4**, suitable for X-ray diffraction analysis, formed after ten days. Yield: 17 mg (26%, based on the metal salt). Elemental analysis (%) calcd for $C_{38}H_{56}Tm_2N_6O_{20}S_2$: C 34.61, H 4.28, N 6.37; found C 34.45, H 4.16, N 6.64. IR (KBr, cm^{-1}): 1619(m), 1542(s), 1434(s), 1395 (m), 1329 (m), 1304 (m), 1231 (m), 1204(w), 1149 (m), 1126 (m), 1077 (w), 1043(m), 1018 (m), 980 (w), 960 (w), 941 (w), 890 (m), 855(w), 794 (w), 760(m), 749 (m), 737 (m), 701(w), 676 (m), 649 (m), 633 (w), 590 (w).

$[Yb_2L_2(OAc)_4(MeOH)_2]\cdot[Yb_2L_2(OAc)_4(H_2O)_2]\cdot 4H_2O$ (5)

$Yb(OAc)_3\cdot 6H_2O$ (0.1 mmol, 90.83 mg) was reacted with HL (0.1 mmol, 25.93 mg) in MeOH/DMF (20 mL/2 mL) in the presence of Et_3N (0.15 mmol, 0.15 mL). The ensuing yellow solution was stirred for 5 h and subsequently filtered. The filtrate was left undisturbed to allow the slow volatilization of the solvent. Yellow block-shaped single crystals of complex **5**, suitable for X-ray diffraction analysis, formed after two weeks. Yield: 23 mg (18%, based on the metal salt). Elemental analysis (%) calcd for $C_{70}H_{84}Yb_4N_{12}O_{28}S_4$: C 34.66, H 3.49, N 6.93; found C 34.42, H 3.36, N 6.98. IR (KBr, cm^{-1}): 1615 (m), 1534 (s), 1477 (w), 1442 (m), 1386 (m), 1346 (w), 1329 (m), 1232 (m), 1203 (m), 1153 (m), 1126 (m), 1079 (w), 1026 (w), 958 (w), 893 (m), 848 (w), 807 (w), 750 (m), 697 (w), 674 (m).

Results and discussion

A dinuclear Dy_2 complex bridged by n-butyric acid groups in the form of $\eta^1:\eta^2:\mu_2$ has been previously reported by S. K. Ghosh and coworkers.[14b] Both complex **3** and this reported complex are bridged by bidentate carboxylate groups, as shown in Scheme 1. However, different from complex **3** with observable relaxation maxima, only temperature dependence was observed in the reported structure, which is probably due to the differences in coordination geometry of the dysprosium centre in respective structures.

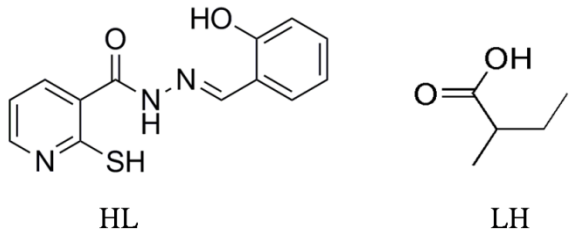

HL LH

Scheme 1 Schematic diagram of ligands used in complexes **1-5** (left) and Dy_2 (right, ref. 14*b*).

Crystal Structures of 1-5

The single-crystal X-ray diffraction studies revealed that all complexes are crystallized in the triclinic space group *P*-1 with $Z = 1$. The molecular structures of **3-5** are depicted in Fig. 1. Crystal data and structure refinement details are summarized in Table 1 and selected bond lengths and bond angles are listed in Table 2.

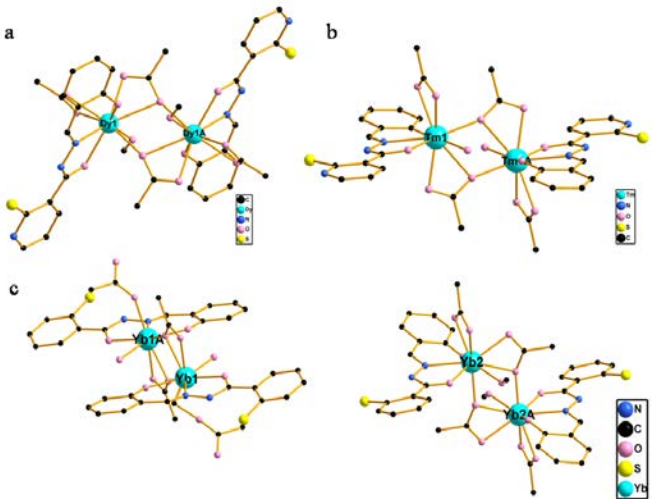

Fig. 1 Partially labeled centrosymmetric units of complexes **3** (a), **4** (b), and **5** (c) with solvents and hydrogen atoms omitted for clarity.

As shown in Fig. 1, all five complexes are centrosymmetric and share the similar dinuclear core structure, where each metal ion is located in the chelating pocket formed by the carboxyl-O, phenol-O, and hydrazide-N from the HL (Fig. 2a). The metal centres are bridged by the acetate groups (O6 and O6A) in the form of $\eta^1:\eta^2:\mu_2$, with the Ln-Ln distance being 4.0128(12) to 4.1802(10) Å and the Ln1-O6-Ln1A angles between 111.2(2)° and 113.52(12)°. For all complexes, the coordination geometry of Ln ions was calculated by utilizing the SHAPE 2.1 software[21] (Table S1 in ESI) and the representative coordination polyhedra are shown in Fig. S1 (see ESI). The Ln ions in complexes **1-4** and the Yb2 in **5** are nine-coordinated and exhibit distorted mono-capped square antiprismatic geometry, while the eight-coordinated Yb1 in **5** exhibits triangular dodecahedron (Fig. S1 in ESI). In complexes **1-3**, the coordination sphere of Ln is completed by two acetate ions and two methanol molecules (Fig. 1a), while the Ln ion in **4** is coordinated by two acetate groups and two H_2O molecules (Fig. 1b).

There are three coordination modes of the acetate groups in complexes **1-5**, as $\eta^1:\eta^2:\mu_2$, η^2 and η^1, which are shown in Fig. 2b. Furthermore, examinations of the crystal packing (Fig. S2 in ESI)) reveal that the molecules are stacked in a parallel manner, producing a framework where the shortest intermolecular Ln-Ln distances for in and between the parallel lines are summarized in Table S2 (see ESI).

In contrast, the two metal centres are bridged by two carboxylate oxygens from two different ligands in an anti-parallel way with Dy-Dy separation distance of 4.074 Å and Dy-O-Dy angle of 113.1° in the previously reported Dy_2 complex.[14b] Though the Dy ions are nine-coordinated and reside in the symmetrical coordination environment like that in **3**, each Dy centre is filled by a purely O_9 donor set. Close analysis of the resulting data utilizing SHAPE 2.1 software reveals that the values obtained are 2.097 and 1.197 (Table S1 in ESI) for complex Dy_2 in ref. 14*b* and **3** respectively, both deviating from zero (zero represents the case of the ideal geometry considered). The coordination geometry of Dy ion in complex **3** is more closed to ideal monocapped square antiprism, which may afford stronger magnetic anisotropy. The molecular structures of two complexes are shown in Fig. S3 (see ESI) with the main bond lengths and bond angles are labeled.

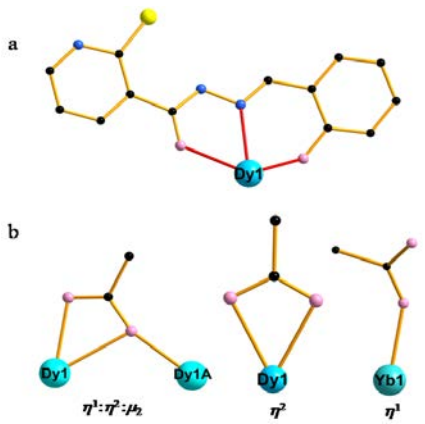

Fig. 2 (a) Connection mode of HL ligand and (b) three specific coordinate modes of acetate groups: $\eta^1:\eta^2:\mu_2$, η^2 and η^1.

Magnetic properties

Magnetic measurements were performed on polycrystalline samples of **2-5**. The phase purity of the bulk samples is confirmed by XRD analyses as shown in Fig. S4. Direct current (dc) magnetic susceptibility studies of the samples in an applied magnetic field of 1000 Oe between 300 and 1.9 K are shown in Fig. 3 in the form of $\chi_M T$ versus T, where χ_M is the molar magnetic susceptibility. Partial of the dc magnetic data of **2-5** are summarized in Table 3. The observed $\chi_M T$ products at room temperature (300 K) are in good agreement with the expected values for two non-interacting two Ln ions.

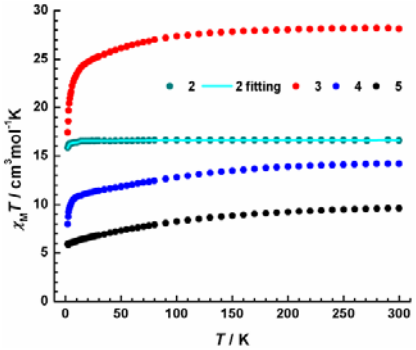

Fig. 3 Plots of $\chi_M T$ versus T for **2**-**5** (with χ_M being the molar susceptibility defined as M/H) in a dc field of 1000 Oe (1.9-300 K). The light-blue solid line corresponds to the best fit using MAGPACK program.

Firstly, we focus on complex **2**, as the isotropic f^7 Gd ion has no orbital contribution. The $\chi_M T$ value of **2** at 300 K is 16.62 cm^3 K mol^{-1}, which is consistent with the spin only value of 15.75 cm^3 K mol^{-1} expected for two non-interacting Gd ions (S = 7/2, L = 0, $^8S_{7/2}$, g = 2: C = 7.875 cm^3 K mol^{-1}).[7a] As temperature decreased, the $\chi_M T$ values are almost constant to 14 K, and decrease to reach 15.66 cm^3 K mol^{-1} at 2 K. This behaviour is indicative of the presence of very weak antiferromagnetic interactions between the Gd ions within the Gd_2 complex. The $\chi_M T$ versus T data were simulated using MAGPACK program[22] based on spin-only Hamiltonian $\hat{H} = -2J\hat{S}_{Gd1} \cdot S_{Gd1A}$ (solid line), giving the best-fit parameters J = -0.01 cm^{-1}, g = 2.06, which is consistent with the results that very weak magnetic interactions is operating in Gd complex.[23]

Table 1 Crystallographic data and structure refinement for complexes **1**-**5**.

Complex	**1**	**2**	**3**	**4**	**5**
Formula	$C_{38}H_{48}Sm_2N_6O_{16}S_2$	$C_{38}H_{48}Gd_2N_6O_{16}S_2$	$C_{38}H_{48}Dy_2N_6O_{16}S_2$	$C_{38}H_{56}Tm_2N_6O_{20}S_2$	$C_{70}H_{84}Yb_4N_{12}O_{28}S_4$
Mr	1209.64	1223.44	1233.96	1318.87	2425.89
Colour	yellow blocks	yellow blocks	yellow blocks	yellow blocks	yellow blocks
Crystal system	triclinic	triclinic	triclinic	triclinic	triclinic
Space group	*P*-1	*P*-1	*P*-1	*P*-1	*P*-1
T [K]	293(2)	293(2)	293(2)	293(2)	293(2)
a [Å]	10.447(3)	10.198(11)	10.310(5)	9.3882(12)	10.885(4)
b [Å]	10.886(3)	10.642(11)	10.622(5)	10.9654(14)	12.424 (4)
c [Å]	11.875(3)	11.568(12)	11.674(6)	13.1679(16)	17.847(7)
α [deg]	69.437(5)	69.60(2)	69.650(9)	111.464(2)	70.887(6)
β [deg]	84.878(5)	85.69(2)	85.710(8)	92.422(2)	73.303(6)
γ [deg]	79.669(5)	81.48(2)	81.099(8)	91.767(2)	89.712(6)
V [Å ^{3}]	1243.4(6)	1163(2)	1183.9(10)	1258.9(3)	2173.8(14)
Z	1	1	1	1	1
ρ_{calcd} [g cm^{-3}]	1.615	1.746	1.731	1.740	1.853
μ[mm^{-1}]	2.491	2.989	3.291	3.662	4.447
F(000)	602	606	610	656	1188
R_{int}	0.0360	0.0938	0.0277	0.0209	0.0198
GOF	1.052	0.956	1.024	1.053	1.036
$R1$ [$I > 2\sigma(I)$]	0.0520	0.0922	0.0405	0.0310	0.0302
$wR2$ (all data)	0.1432	0.2195	0.0982	0.0765	0.0751

Table 2 Selected bond lengths (Å) and bond angles (°) for complexes **1-5**.

Complex	**1**	**2**	**3**	**4**	5
Ln(1)-O(6)	2.624(5)	2.602(11)	2.628(4)	2.649(3)	2.342(3)
Ln(1)-O(6A)	2.440(5)	2.340(10)	2.348(4)	2.306(3)	2.477(4)
Ln(1)-O(5)	2.482(6)	2.444(12)	2.411(5)	2.441(3)	2.246(4)
Ln(1)-O(7)	2.465(6)	2.385(13)	2.378(5)	2.332(3)	#
Ln(1)-O(2)	2.328(5)	2.246(10)	2.254(4)	2.220(3)	2.211(4)
Ln(1)-O(1)	2.463(6)	2.399(11)	2.380(4)	2.328(3)	2.324(4)
Ln(1)-O(4)	2.501(6)	2.415(11)	2.419(4)	2.411(4)	2.322(4)
Ln(1)-O(3)	2.501(6)	2.420(12)	2.434(4)	2.528(3)	2.388(4)
Ln(1)-N(3)	2.622(7)	2.553(16)	2.538(5)	2.490(3)	2.476(4)
Ln(1)-Ln(1A)	4.1802(10)	4.0992(35)	4.1245(16)	4.1486(5)	4.0128(12)
Ln(1)-O(6)-Ln(1A)	111.2(2)	112.0(4)	111.86(16)	113.52(12)	112.71(14)
O6-Ln(1)-O6A	68.8 (2)	68.0(4)	68.14(16)	66.48(12)	67.29(14)

Symmetry codes: for **1**, A: -x+1, -y, -z+1; for **2**, A,-x+1, -y, -z+1; for **3**, A, -x+1, -y+1, -z+2; for **4,** A, -x+2, -y+2, -z+1; for **5**, 1A, -x+1, -y, -z+1.

Table 3 Summary of direct current (dc) magnetic data for **2-5**.

complex	**2**	**3**	**4**	**5**
ground state term of Ln ion	$^8S_{7/2}$	$^6H_{15/2}$	$^3H_6$	$^2F_{7/2}$
C (cm^3 K mol^{-1}) for each Ln ion	7.875	14.17	7.15	2.57
χT (cm^3 K mol^{-1}) expected value for Ln_2 at RT	15.75	28.34	14.30	5.14
χT (cm^3 K mol^{-1}) experimental value for Ln_2 at RT	16.62	28.13	14.22	4.84
χT (cm^3 K mol^{-1}) experimental value for Ln_2 at 2.0 K	15.66	17.40	7.79	2.78

The temperature dependence of the magnetic susceptibilities for complexes **3-5** show similar thermal evolution at high temperature region. For **3** and **4**, the $\chi_M T$ product at 1000 Oe is essentially temperature independent over the range 300-100 K, followed by a slightly decrease on lowering the temperature from 100 to 20 K and then rapidly decreases to reach a minimum of 17.50 cm^3 K mol^{-1} and 7.79 cm^3 K mol^{-1} at about 2 K. For **5** the $\chi_M T$ product begins a very slow decrease at higher temperature like other complexes, but without abrupt decrease below 100 K. The Stark sublevels of the anisotropic Ln (Dy, Tm and Yb) ions are thermally depopulated when the temperature is lowered, resulting in a decrease of the $\chi_M T$ product. Therefore, the decrease is most likely ascribed to the progressive depopulation of excited Stark sublevels, significant magnetic anisotropy and/or weak antiferromagnetic interactions present in these systems.[24]

The field dependence of the magnetization of complexes **3** and **5** at low temperatures shows that the magnetization increases smoothly with increasing applied dc field without saturation even at 7 T (Fig. S5 in ESI), which is most likely due to anisotropy and important crystal-field effect at the metal ions. Furthermore, the absence of a superposition of the *M* versus *H*/*T* data on a single master-curve for **3** and **5** (Fig. 4), suggesting the presence of significant magnetic anisotropy and/or low-lying excited states in the systems. In addition, the absence of the hysteresis loop above 1.9 K (Fig. S6 in ESI) in the complex **3** may be caused by the presence of a relatively fast zero-field relaxation.

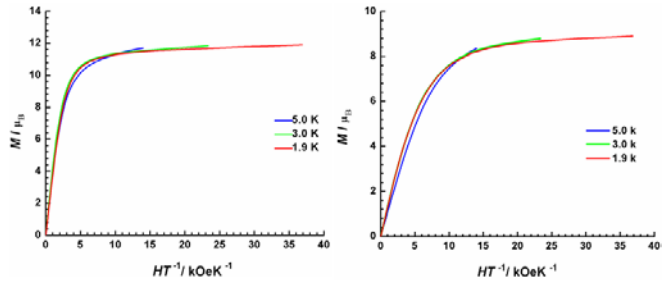

Fig. 4 Field dependence of magnetizations of **3** (left) and **5** (right) at different temperatures below 5 K.

To probe the dynamics of the magnetization, alternating current susceptibility measurements were carried out under zero field. Both in-phase (χ') and out-of-phase (χ'') alternating current (ac) susceptibilities for the complex **3** exhibit temperature and frequency dependences. The slow relaxation of the magnetization signals typical features associated with SMM behaviour. As shown in Fig. 5 and Fig. S7 in ESI, χ' shows the maxima in the 7-13 K, while the χ'' define maxima between 5 K (50 Hz) and 13 K(1500 Hz). Unlike most Ln-SMM, the absence of another increase in the low-temperature in both χ' and χ'' compounds for **3** indicates the efficient suppression of zero-field tunneling of magnetization.[25] In contrast, Dy_2 in ref. 14*b* complex only shows temperature dependence but without observable maxima (Fig. 5, right). Thus complex **3** show prominent SMM behaviour. The obvious disparity in magnetic dynamics should mainly result from the more distorted coordination geometry in the Dy_2 in ref. 14*b*, thus leading to the fast quantum tunneling from more transverse anisotropy.

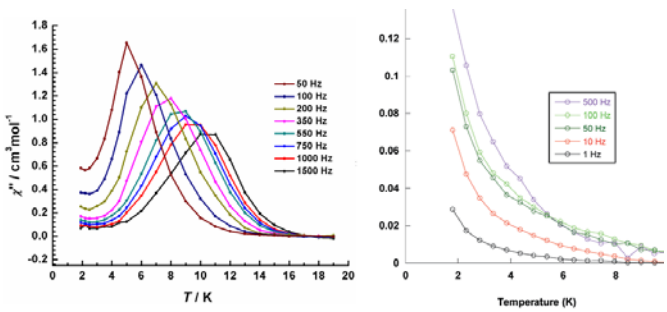

Fig. 5 Temperature dependence of the out-of-phase (χ'') of the ac susceptibility for **3** (left) and Dy_2 (right, ref. 14*b*) under zero-dc field. The solid lines are guides for the eyes.

As shown in Fig. 6, in the range of 1.9 K to 10 K, we can observe the peaks of χ'', and these peaks move gradually to high frequencies with the increase of temperature. Besides, ac susceptibilities were also measured under various magnetic field at 9 K, as shown in Fig.S8 in ESI. The maxima of the frequency-dependent ac signals shift negligibly under various dc fields, which indicates that dc field has insignificant effect on the relaxation and suggests that tunneling in zero field is not an efficient pathway at 9 K.

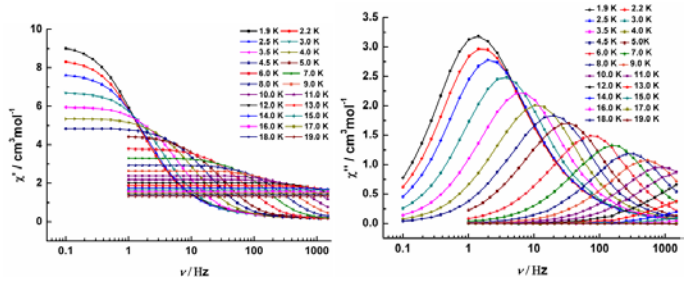

Fig. 6 Frequency dependence of the in-phase (χ') and out-of-phase (χ'') of the ac susceptibility for **3** under zero-dc field. The solid lines are guides for the eyes.

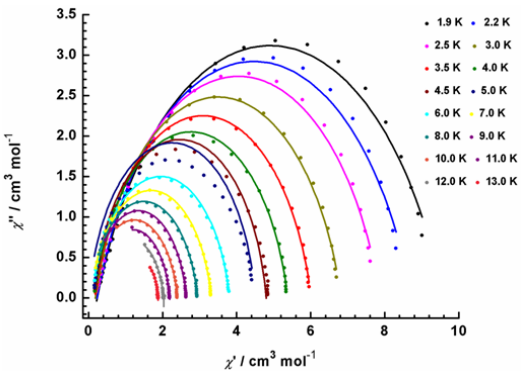

Fig. 7 Cole-Cole plots measured at 1.9 K-14 K under zero-dc field for **3**. The solid lines are the best fits to the experimental data, obtained with the generalized Debye model[2a, 26] with α parameters below 0.30.

For complex **3**, Cole-Cole plots plotted as the in-phase *vs.* out-of-phase ac susceptibility data show an asymmetrical semi-circular shape (Fig. 7), which can be fitted by the generalized Debye model, with α parameters below 0.30 from 1.9 to 13.0 K (Table S4 in ESI), indicating a narrow distribution of relaxation time.[26a]

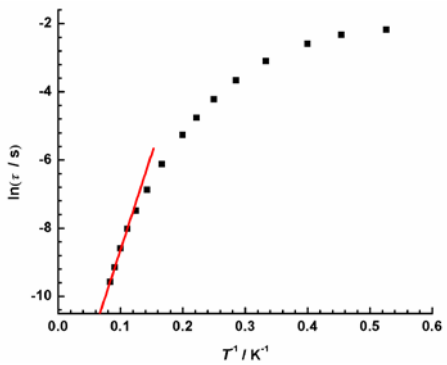

Fig. 8 Magnetization relaxation time, lnτ, versus T^{-1} plot for **3** under zero-dc field. The solid line is fitted with the Arrhenius law.

The magnetization relaxation time (τ) has been extracted from frequency dependencies of the ac susceptibility between 1.9 and 13 K (Fig. 8). Above 7 K, the relaxation follows a thermally activated mechanism and the Arrhenius plot of lnτ versus 1/*T*, where τ is the relaxation time constant, is linear (Fig.8). The plot can be fitted by the Arrhenius law [$\tau = \tau_0 \exp(U_{eff}/k_BT)$] and afford an anisotropic energy barrier (U_{eff}) of 39.1 K and a pre-exponential factor (τ_0) of 6.4×10^{-7} s. These parameters are comparable to those reported for other SMMs.[13]

Below 7 K, τ becomes weakly dependent on *T* as the temperature decreases, indicating a gradual crossover from a thermally activated Orbach mechanism that is predominant at higher temperatures (red line), to a direct or phonon induced tunnelling process at lower temperatures.

Conclusion

In summary, we described here a new family of dinuclear Ln complexes obtained by the reaction of $Ln(OAc)_3 \cdot 6H_2O$ with Schiff base ligands. The two metals in the dinuclear core in each compound are bridged by acetate groups in the form of $\eta^1:\eta^2:\mu_2$. These complexes were investigated by SHAPE 2.1 software and magnetic studies. Compared with Dy_2 in ref. 14*b*, complex **3** exhibits SMM behaviour with energy barrier of 39.1 K due to its less distorted coordination geometry around Dy. The simple comparative investigations may get insight into the structure-property relationship of lanthanide-based SMMs, which is crucial to the advancement of single-molecule data storage and processing technologies.

Acknowledgements

We thank the National Natural Science Foundation of China (21241006, 21221061 and 21371166) for financial support.

Notes and references

[a] State Key Laboratory of Rare Earth Resource Utilization, Changchun Institute of Applied Chemistry, Chinese Academy of Sciences, Changchun, 130022, China. E-mail: tang@ciac.ac.cn; Fax: +86 431 85262878; Tel: +86 431 85262878

[b] University of Chinese Academy of Sciences, Beijing 100049, China

1. (a) R. Sessoli, H. L. Tsai, A. R. Schake, S. Y. Wang, J. B. Vincent, K. Folting, D. Gatteschi, G. Christou and D. N. Hendrickson, *J. Am. Chem. Soc.*, 1993, **115**, 1804-1816; (b) R. Sessoli, D. Gatteschi, A. Caneschi and M. A. Novak, *Nature*, 1993, **365**, 141-143.
2. (a) D. Gatteschi, R. Sessoli and J. Villain, *Oxford University Press:Oxford, U.K.*, 2006; (b) D. Gatteschi and R. Sessoli, *Angew. Chem., Int. Ed.*, 2003, **42**, 268-297; (c) Y. N. Guo, G. F. Xu, P. Gamez, L. Zhao, S. Y. Lin, R. P. Deng, J. K. Tang and H. J. Zhang, *J. Am. Chem. Soc.*, 2010, **132**, 8538-8539; (d) M. N. Leuenberger and D. Loss, *Nature*, 2001, **410**, 789-793.
3. D. Gatteschi, A. Caneschi, L. Pardi and R. Sessoli, *Science*, 1994, **265**, 1054-1058.
4. N. Roch, S. Florens, V. Bouchiat, W. Wernsdorfer and F. Balestro, *Nature*, 2008, **453**, 633-U633.
5. E. Coronado and P. Day, *Chem. Rev.*, 2004, **104**, 5419-5448.
6. (a) G. Aromi and E. K. Brechin, in *Single-Molecule Magnets and Related Phenomena*, ed. R. Winpenny, 2006, pp. 1-67; (b) C. J. Milios, A. Vinslava, W. Wernsdorfer, S. Moggach, S. Parsons, S. P. Perlepes, G. Christou and E. K. Brechin, *J. Am. Chem. Soc.*, 2007, **129**, 2754-2755; (c) H. Miyasaka, R. Clerac, W. Wernsdorfer, L. Lecren, C. Bonhomme, K. Sugiura and M. Yamashita, *Angew. Chem., Int. Ed.*, 2004, **43**, 2801-2805.
7. (a) C. Benelli and D. Gatteschi, *Chem. Rev.*, 2002, **102**, 2369-2387; (b) A. Bencini, C. Benelli, A. Caneschi, R. L. Carlin, A. Dei and D. Gatteschi, *J. Am. Chem. Soc.*, 1985, **107**, 8128-8136; (c) O. Guillou, P. Bergerat, O. Kahn, E. Bakalbassis, K. Boubekeur, P. Batail and M. Guillot, *Inorg. Chem.*, 1992, **31**, 110-114.
8. C. Benelli, A. Caneschi, D. Gatteschi and R. Sessoli, *Adv. Mater.*, 1992, **4**, 504-505.
9. (a) R. Sessoli and A. K. Powell, *Coord. Chem. Rev.*, 2009, **253**, 2328-2341; (b) L. F. Zou, L. Zhao, Y. N. Guo, G. M. Yu, Y. Guo, J. K. Tang and Y. H. Li, *Chem. Commun.*, 2011, **47**, 8659-8661.
10. (a) S. Y. Lin, L. Zhao, Y. N. Guo, P. Zhang, Y. Guo and J. K. Tang, *Inorg. Chem.*, 2012, **51**, 10522-10528; (b) L. Sorace, C. Benelli and D. Gatteschi, *Chem. Soc. Rev.*, 2011, **40**, 3092-3104; (c) J. K. Tang, I. Hewitt, N. T. Madhu, G. Chastanet, W. Wernsdorfer, C. E. Anson, C. Benelli, R. Sessoli and A. K. Powell, *Angew. Chem., Int. Ed.*, 2006, **45**, 1729-1733.
11. (a) J. Long, F. Habib, P.-H. Lin, I. Korobkov, G. Enright, L. Ungur, W. Wernsdorfer, L. F. Chibotaru and M. Murugesu, *J. Am. Chem. Soc.*, 2011, **133**, 5319-5328; (b) J. D. Rinehart, M. Fang, W. J. Evans and J. R. Long, *Nat. Chem.*, 2011, **3**, 538-542; (c) J. D. Rinehart, M. Fang, W. J. Evans and J. R. Long, *J. Am. Chem. Soc.*, 2011, **133**, 14236-14239; (d) R. J. Blagg, C. A. Muryn, E. J. L. McInnes, F. Tuna and R. E. P. Winpenny, *Angew. Chem., Int. Ed.*, 2011, **50**, 6530-6533; (e) N. Ishikawa, M. Sugita, T. Ishikawa, S. Koshihara and Y. Kaizu, *J. Am. Chem. Soc.*, 2003, **125**, 8694-8695; (f) M. Gonidec, R. Biagi, V. Corradini, F. Moro, V. De Renzi, U. del Pennino, D. Summa, L. Muccioli, C. Zannoni, D. B. Amabilino and J. Veciana, *J. Am. Chem. Soc.*, 2011, **133**, 6603-6612; (g) R. J. Blagg, L. Ungur, F. Tuna, J. Speak, P. Comar, D. Collison, W. Wernsdorfer, E. J. L. McInnes, L. F. Chibotaru and R. E. P. Winpenny, *Nat. Chem.*, 2013, **5**, 673-678.
12. (a) L. E. Roy and T. Hughbanks, *J. Am. Chem. Soc.*, 2006, **128**, 568-575; (b) J.-B. Peng, X.-J. Kong, Y.-P. Ren, L.-S. Long, R.-B. Huang and L.-S. Zheng, *Inorg. Chem.*, 2012, **51**, 2186-2190; (c) S. Mukherjee, A. K. Chaudhari, S. Xue, J. Tang and S. K. Ghosh, *Inorg. Chem. Commun.*, 2013, **35**, 144-148.
13. F. Tuna, C. A. Smith, M. Bodensteiner, L. Ungur, L. F. Chibotaru, E. J. L. McInnes, R. E. P. Winpenny, D. Collison and R. A. Layfield, *Angew. Chem., Int. Ed.*, 2012, **51**, 6976-6980.
14. (a) Y. Z. Zheng, Y. Lan, W. Wernsdorfer, C. E. Anson and A. K. Powell, *Chem.- Eur. J.*, 2009, **15**, 12566-12570; (b) S. K. Ghosh, B. Joarder, A. K. Chaudhari and G. Rogez, *Dalton Trans.*, 2012, **41**, 7695; (c) L. Liang, G. Peng, G. Li, Y. Lan, A. K. Powell and H. Deng, *Dalton Trans.*, 2012, **41**, 5816-5823; (d) Y. M. Song, F. Luo, M. B. Luo, Z. W. Liao, G. M. Sun, X. Z. Tian, Y. Zhu, Z. J. Yuan, S. J. Liu, W. Y. Xu and X. F. Feng, *Chem Commun.*, 2012, **48**, 1006-1008.
15. P. Zhang, L. Zhang, S. Y. Lin, S. F. Xue and J. K. Tang, *Inorg. Chem.*, 2013, **52**, 4587-4592.
16. B. Hussain, D. Savard, T. J. Burchell, W. Wernsdorfer and M. Murugesu, *Chem. Commun.*, 2009, 1100-1102.
17. (a) S. Xue, L. Zhao, Y.-N. Guo, X.-H. Chen and J. Tang, *Chem Commun.*, 2012 **48**, 7031-7033; (b) Y. N. Guo, G. F. Xu, W. Wernsdorfer, L. Ungur, Y. Guo, J. K. Tang, H. J. Zhang, L. F. Chibotaru and A. K. Powell, *J. Am. Chem. Soc.*, 2011, **133**, 11948-11951; (c) S.-Y. Lin, W. Wernsdorfer, L. Ungur, A. K. Powell, Y.-N. Guo, J. Tang, L. Zhao, L. F. Chibotaru and H.-J. Zhang, *Angew. Chem., Int. Ed.*, 2012, **51**, 12767-12771.

18. (a) M. Diop, F. B. Tamboura, M. Gaye, A. S. Sall, A. H. Barry and T. Jouini, *B. Chem. Soc. Ethiopia*, 2003, **17**, 167-172; (b) X. H. Bu, M. Du, L. Zhang, X. B. Song, R. H. Zhang and T. Clifford, *Inorg Chim Acta*, 2000, **308**, 143-149.
19. E. A. Boudreaux and L. N. Mulay, *John Wiley & Sons, New York*, 1976.
20. (a) G. M. Sheldrick, *SHELXS-97, Program for Crystal Structure Solution*, University of Göttingen, Germany, 1997; (b) G. M. Sheldrick, *SHELXL-97. Program for Crystal Structure Refinement*, University of Göttingen, Germany, 1997.
21. D. Casanova, M. Llunell, P. Alemany and S. Alvarez, *Chem.-Eur. J.*, 2005, **11**, 1479-1494.
22. J. J. Borras-Almenar, J. M. Clemente-Juan, E. Coronado and B. S. Tsukerblat, *Inorg. Chem.*, 1999, **38**, 6081-6088.
23. Y. Wang, X.-L. Li, T.-W. Wang, Y. Song and X.-Z. You, *Inorg. Chem*, 2010, **49**, 969-976.
24. (a) M. L. Kahn, R. Ballou, P. Porcher, O. Kahn and J. P. Sutter, *Chem.-Eur. J.*, 2002, **8**, 525-531; (b) M. L. Kahn, J. P. Sutter, S. Golhen, P. Guionneau, L. Ouahab, O. Kahn and D. Chasseau, *J. Am. Chem. Soc.*, 2000, **122**, 3413-3421.
25. (a) P. H. Lin, T. J. Burchell, R. Clérac and M. Murugesu, *Angew. Chem., Int. Ed.*, 2008, **47**, 8848-8851; (b) G. F. Xu, Q. L. Wang, P. Gamez, Y. Ma, R. Clerac, J. K. Tang, S. P. Yan, P. Cheng and D. Z. Liao, *Chem. Commun.*, 2010, **46**, 1506-1508.
26. (a) K. S. Cole and R. H. Cole, *J. Chem. Phys.*, 1941, **9**, 341-351; (b) S. M. J. Aubin, Z. M. Sun, L. Pardi, J. Krzystek, K. Folting, L. C. Brunel, A. L. Rheingold, G. Christou and D. N. Hendrickson, *Inorg.Chem.*, 1999, **38**, 5329-5340.

Graphical Abstract

Five dinuclear Ln complexes bridged by acetate groups in the form of $\eta^1:\eta^2:\mu_2$ mode were reported with the Dy_2 analogue behaves as SMM.